Available online at www.sciencedirect.com
SCIENCE DIRECT®
Journal of Sound and Vibration 284 (2005) 1099–1118
JOURNAL OF SOUND AND VIBRATION
www.elsevier.com/locate/jsvi

Circulation pumps as structure-borne sound sources: emission to finite pipe systems

B.M. Gibbs*, N. Qi

Acoustics Research Unit, School of Architecture and Building Engineering, University of Liverpool, Liverpool L69 3BX, UK

Received 18 December 2003; received in revised form 29 July 2004; accepted 29 July 2004
Available online 13 December 2004

Abstract

In a recent paper, it was shown that the structure-borne sound power from circulation pumps into straight pipes is primarily through the translation components, which generate longitudinal and bending waves. In this paper, the subsequent wave mode conversions at pipe junctions are considered. A central heating system was physically modelled as various combinations of pipes with a radiator. The experimental measurements were of fixed pipe lengths and resonance effects dominated the system response. In addition, small misalignments increased wave mode conversion. In order to consider only the effect of number and orientation of pipe junctions, an idealised pipe system was modelled such that the length of the connecting pipes could be varied stochastically, thereby randomising out resonance effects. For typically domestic pipe systems the mixing of wave types is such that the radiated sound is determined by the largest component of the structure-borne power from the pump into the pipe system, irrespective of the direction.

1. Introduction

Circulation pumps are the principal active component in pipe systems and complaints of excessive noise in domestic central heating systems often result from them. Problems are seldom due to pumps radiating sound directly into the air [1]. The noise results primarily from liquid-borne sound transmission through the connecting pipe and radiator systems and structure-borne sound transmission

*Corresponding author. Tel.: +44 151 794 4937; fax: +44 151 794 2605.
E-mail address: bmg@liverpool.ac.uk (B.M. Gibbs).

0022-460X/$ - see front matter © 2004 Elsevier Ltd. All rights reserved.
doi:10.1016/j.jsv.2004.07.017

that directly excites the pipe walls, and thus the connected radiators and room surfaces at support points. Therefore, the radiated sound is determined by the installation as well as by the pump. Although there has been a large body of work on liquid-borne noise, leading to standards [2–4], there has been relatively little on the structure-borne component [5]. The overall aim of the work, reported in this paper, was to identify the vibration generating and transmission mechanisms in domestic pumped water systems that cause annoyance and then to develop appropriate test methods for the pumps.

In a companion paper, which considered structure-borne emission into semi-infinite pipes [6], it was shown that at low frequencies and for straight pipes the total power can be described in terms of the torsional, longitudinal, bending, as well as liquid pressure waves. An anechoic structure-borne power can be calculated from the measured free velocity and mobility of the pump for each component of vibration and from receiver mobilities of idealised semi-infinite pipes. For the in-line pumps examined, the three moment-induced power components, which generate a torsional wave and contribute to the bending waves, are much lower than the force-induced power components and can be neglected.

In this paper, the emission into finite pipe systems is examined by considering wave propagation and mode conversions at pipe junctions and other discontinuities. A central heating system was physically modelled as various combinations of pipes with a radiator. In addition, an analytical model of idealised pipe systems was developed where the length of the connecting pipes could be varied stochastically to average out resonance effects such that the effects of number and geometry of pipe junctions could be examined.

2. Experimental investigation

The objective of the experimental investigation was to assess the relative importance of three translational components of power into the free end of pipe systems and thereby assess the effect of the number and orientation of pipe junctions on wave mode transformation. Pipe–radiator systems were assembled from standard copper piping, 22 mm diameter and 0.9 mm wall thickness. The pipes were joined to form right-angle bends. All pipe combinations terminated in a single-panel radiator of dimensions $660 \times 500 \times 25$ mm.The assemblies were elastically suspended. Fig. 1 shows the configurations of the pipe–radiator systems assembled, in order of increasing complexity; from a two-pipe–radiator system, to one composed of three mutually perpendicular pipes. In Figs. 1(a) and (b), the radiator is perpendicular to the plane of the two and three pipes, respectively. In Fig. 1(c), the radiator is parallel with the direction of pipe 2.

An electro-dynamic shaker generated a force into the free end of a pipe through a force transducer (Fig. 2). An accelerometer, in line with the force transducer, registered the response velocity and thus the power into the pipe was obtained. The shaker could be orientated into each of the three required mutually perpendicular directions. The system energy was assumed to be concentrated in the bending field generated on the terminating radiator (Fig. 2).

The contributions of the three input powers $P_{\mathrm{in}_x}, P_{\mathrm{in}_y}, P_{\mathrm{in}_z}$ can be expressed in terms of power transmission coefficients $\gamma_{P_{\mathrm{in}x}}^{P_{rx}}, \gamma_{P_{\mathrm{in}y}}^{P_{ry}}$, and $\gamma_{P_{\mathrm{in}z}}^{P_{rz}}$, defined as:

$$\gamma_{P_{\mathrm{in}x}}^{P_{rx}} = \frac{P_{rx}}{P_{\mathrm{in}x}}, \quad \gamma_{P_{\mathrm{in}y}}^{P_{ry}} = \frac{P_{ry}}{P_{\mathrm{in}y}}, \quad \gamma_{P_{\mathrm{in}z}}^{P_{rz}} = \frac{P_{rz}}{P_{\mathrm{in}z}}, \tag{1}$$

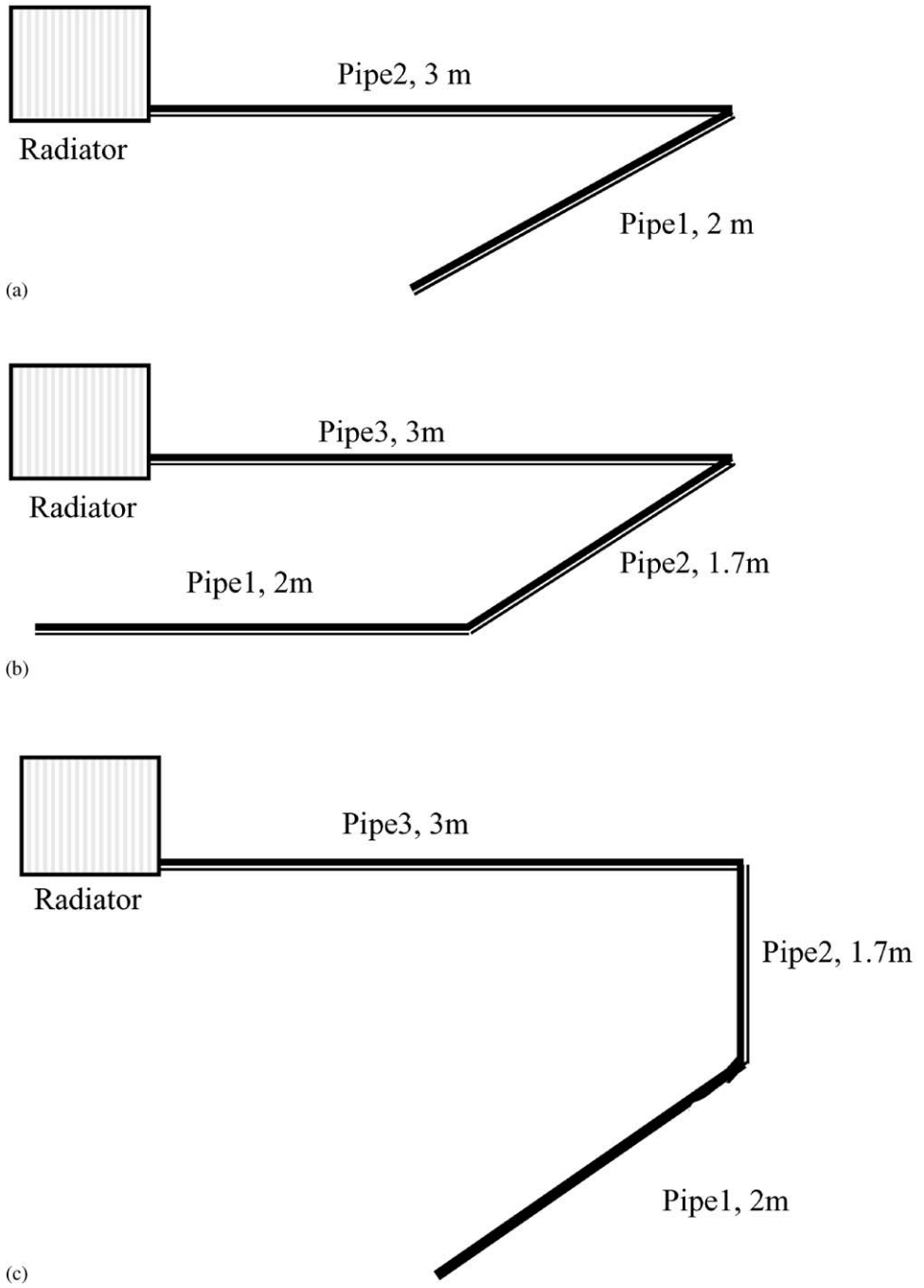

Fig. 1. Experimental pipe–radiator set-up, with dimensions: (a) two pipe system; (b) three pipes in the same plane; (c) three pipes in three mutually perpendicular directions.

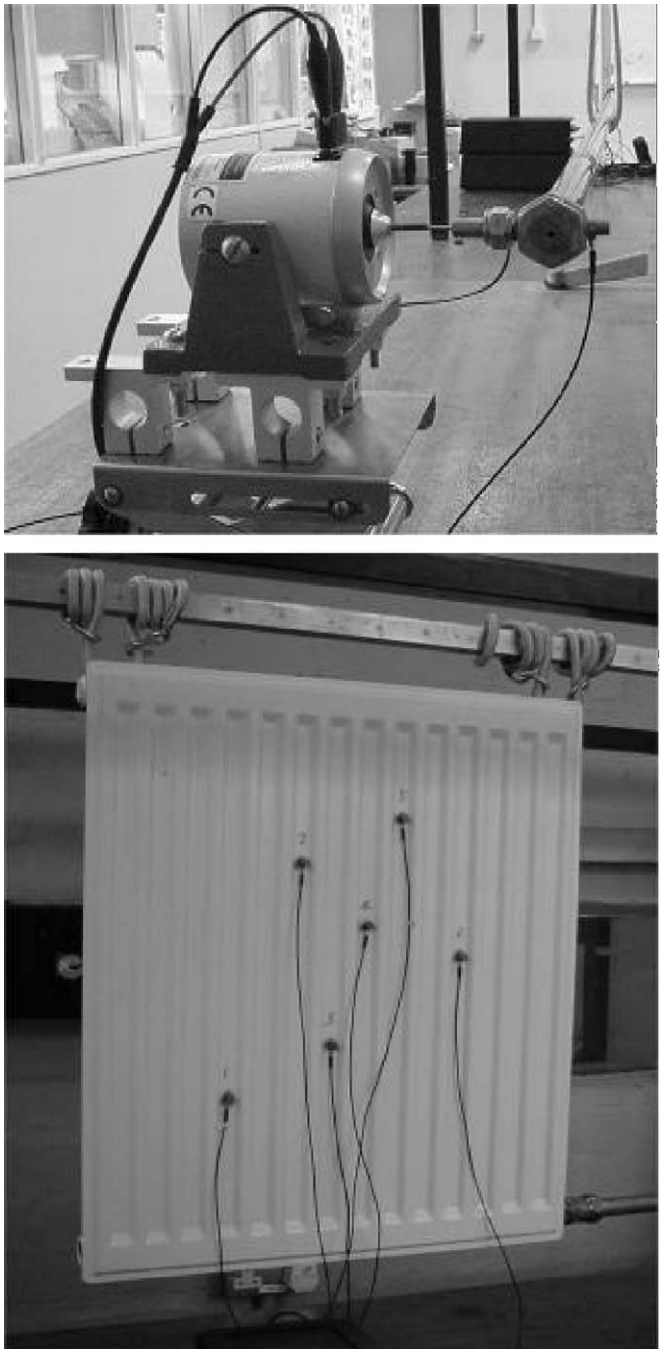

Fig. 2. Set-up for measuring input power at the free end of a pipe and for measuring bending wave power on the connected radiator.

where P_{rx}, P_{ry}, P_{rz} is the resultant bending wave field power of the radiator for the pipe excitation component in the x, y, and z directions, respectively.

The time averaged input power for each component of excitation is obtained from [7] as

$$P_{\text{in}} = \int_0^\infty \frac{\text{Im } G(F,a,f)}{\omega}\, \text{d}f, \tag{2}$$

where $G(F,a,f)$ is the one-sided cross spectral density of point force F and acceleration a, ω is angular velocity. The power received, which is of interest, is that which generates a bending wave field on the radiator, since this field couples efficiently with the air. The measured bending wave power is obtained from [8] as

$$P_r = \tfrac{1}{2}\eta\omega\, m\bar{v}_b^2(f), \tag{3}$$

where m is the mass of the radiator, $\bar{v}_b^2(f)$ is the mean-square velocity of the bending wave field over the surface and η is the loss factor. The mean-square velocity was obtained from six accelerometer measurements (Fig. 2). Since the objective was to investigate the relative contributions of the three components of power into the pipe–radiator system, the loss factor was not required and the power to the radiator was assumed to be proportional to mean-square velocity.

3. Measurement results

3.1. Two-pipe system

The measured power transmission coefficients for a two-pipe–radiator system (lay-out as in Fig. 1a) are shown in Fig. 3a. In Fig. 3b are shown the same values normalised with respect to the transmission coefficient for power in the axial direction, in this case the x-direction. This component and that in the y-direction both give rise, after the pipe bend, to a bending wave with displacement perpendicular to the plane of the radiator surface. The power transmission coefficient $\gamma^{P_{rz}}_{P_{\text{inz}}}$, which corresponds to a generated bending wave polarised in the plane of the radiator, has the lowest value.

This can be explained by considering the transmission equation at the connection point of the pipe and radiator [9]

$$P = \frac{1}{2}\frac{\left|v_{\text{pf}}\right|^2}{\left|\tilde{Y}_p + \tilde{Y}_r\right|^2}\, \text{Re}(\tilde{Y}_r), \tag{4}$$

where v_{pf} is the pipe free velocity before connection to the radiator, $\tilde{Y}_p$ the pipe mobility and $\tilde{Y}_r$ is the mobility of the radiator. The expression for power can be rewritten, according to Mondot and Petersson [10], as

$$P = \tilde{S}\tilde{C}_f,$$

where

$$\tilde{S} = \frac{1}{2}\frac{\left|v_{\text{pf}}\right|^2}{\tilde{Y}_p^*}$$

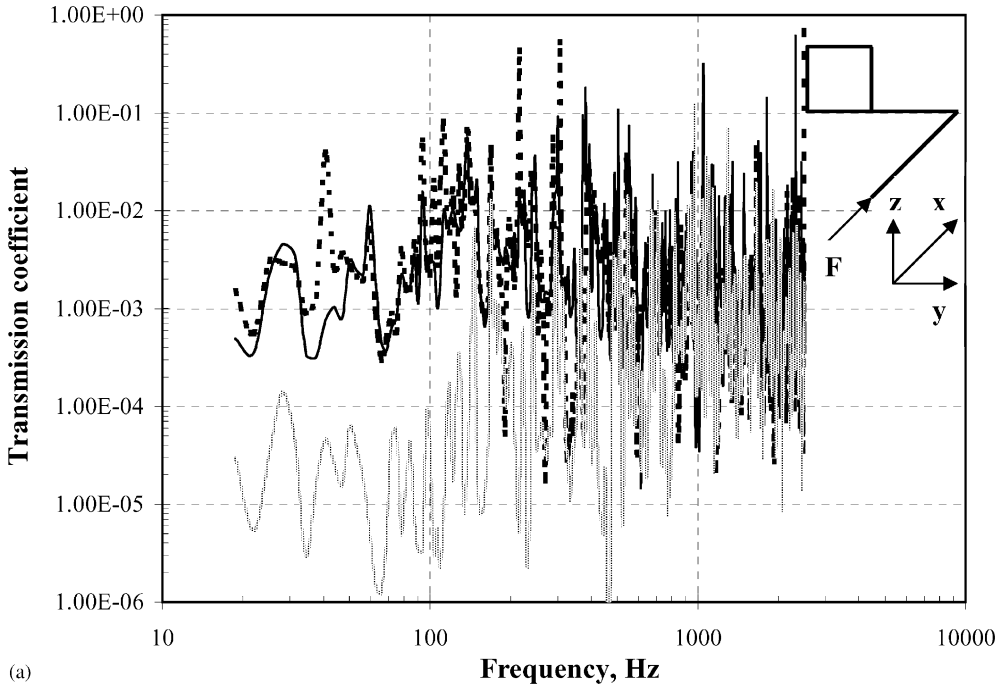

(a)

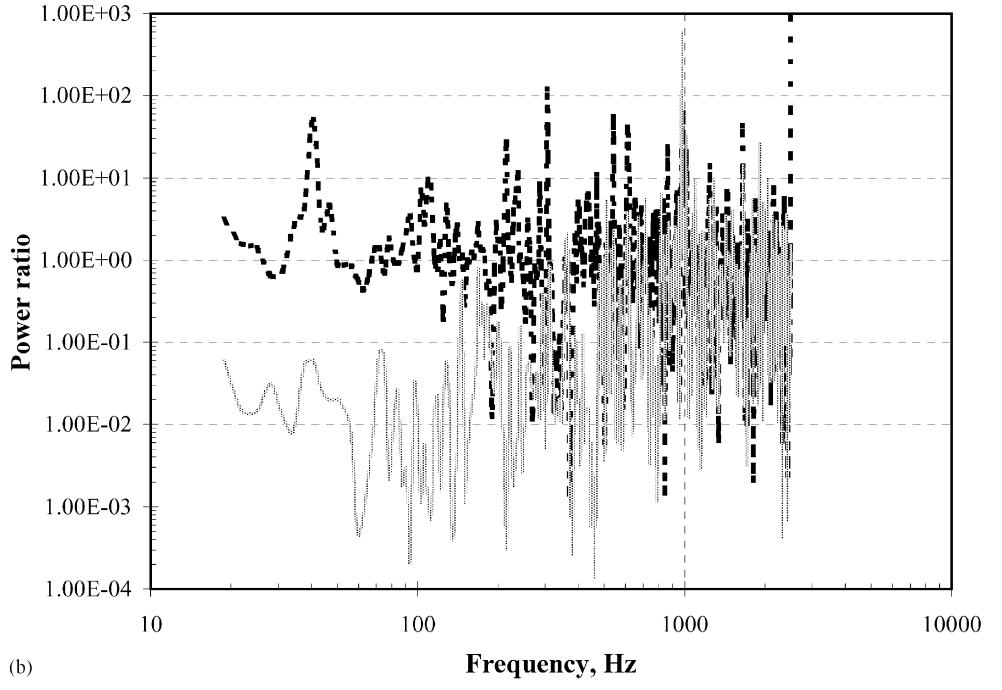

(b)

Fig. 3. (a) Measured transmission coefficients for the two pipe system: ————, $\gamma^{P_{rx}}_{P_{inz}}$; -----, $\gamma^{P_{ry}}_{P_{inz}}$; ————, $\gamma^{P_{rz}}_{P_{inz}}$; (b) normalized values: -----, $\gamma^{P_{ry}}_{P_{iny}}/\gamma^{P_{rx}}_{P_{inx}}$; ————, $\gamma^{P_{rz}}_{P_{inz}}/\gamma^{P_{rx}}_{P_{inx}}$.

and

$$\tilde{C}_f = \frac{\tilde{Y}_p^* \tilde{Y}_r}{\left|\tilde{Y}_p + \tilde{Y}_r\right|^2}, \tag{5}$$

where $\tilde{S}$ is the source descriptor, consisting of pipe properties only, the free velocity at the free end of the pipe and the component mobility. It has units of power. $\tilde{C}_f$ is the coupling function, which expresses the efficiency of the power transmission between pipe and radiator in terms of pipe and radiator mobilities. The coupling functions for three incident waves were obtained from mobilities, given in Table 1, of semi-infinite rods and beams and plates, according to [9]. It was assumed that the in-plane mobilities of the radiator are mass controlled. For the copper pipe: $h = 22\,\text{mm}$, $\rho = 8900\,\text{kg/m}^3$, $c_L = 3900\,\text{m/s}$. For the steel radiator: $h = 25\,\text{mm}$, $\rho = 8003\,\text{kg/m}^3$, $c_L = 5030\,\text{m/s}$.

In Fig. 4 are shown the magnitudes of the coupling function for each component of excitation, at the junction of pipe and radiator, with the coordinate system as given in Table 1. The value of C_{fxx} is consistently greater than that of C_{fyy} and C_{fzz} and corresponds to generation of in-plane waves in the radiator. However, small misalignments at the junction give rise to wave mode conversion, from a longitudinal wave to a bending wave. This has been confirmed experimentally [11,12] and in studies of uncertainty in vibroacoustic behaviour of structures [13] which concluded that misalignments in waveguides, of the order of 4 degrees and less, give rise to significant variations in the coupling of transverse and in-plane motions. The value of C_{fzz} increases with frequency. This, combined with the fact that the incoming bending wave is polarised in the direction perpendicular to the plane of the radiator, results in a significant contribution to the bending wave field on the radiator as indicated by $\gamma^{P_{ry}}_{P_{\text{iny}}}$ in Fig. 3. The value of C_{fyy} is relatively low and corresponds to predominantly in-plane excitation, with a resultant small contribution to the bending field, as indicated by $\gamma^{P_{rz}}_{P_{\text{inz}}}$ in Fig. 3. The increase in transmission coefficients with frequency are in part caused by extraneous wave mode conversions due to imperfections and

Table 1
Mobilities at connection point of pipe and radiator

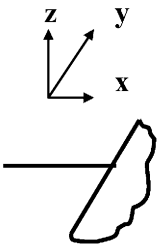	Pipe	Radiator
x-direction	$\dfrac{1}{\rho S c_L}$	$\dfrac{1}{\mathrm{j}\omega M}$
y-direction	$\dfrac{(1-j)}{1.34\rho S\sqrt{c_L h f}}$	$\dfrac{1}{\mathrm{j}\omega M}$
z-direction	$\dfrac{(1-j)}{1.34\rho S\sqrt{c_L h f}}$	$\dfrac{1}{\rho h^2 c_L}$

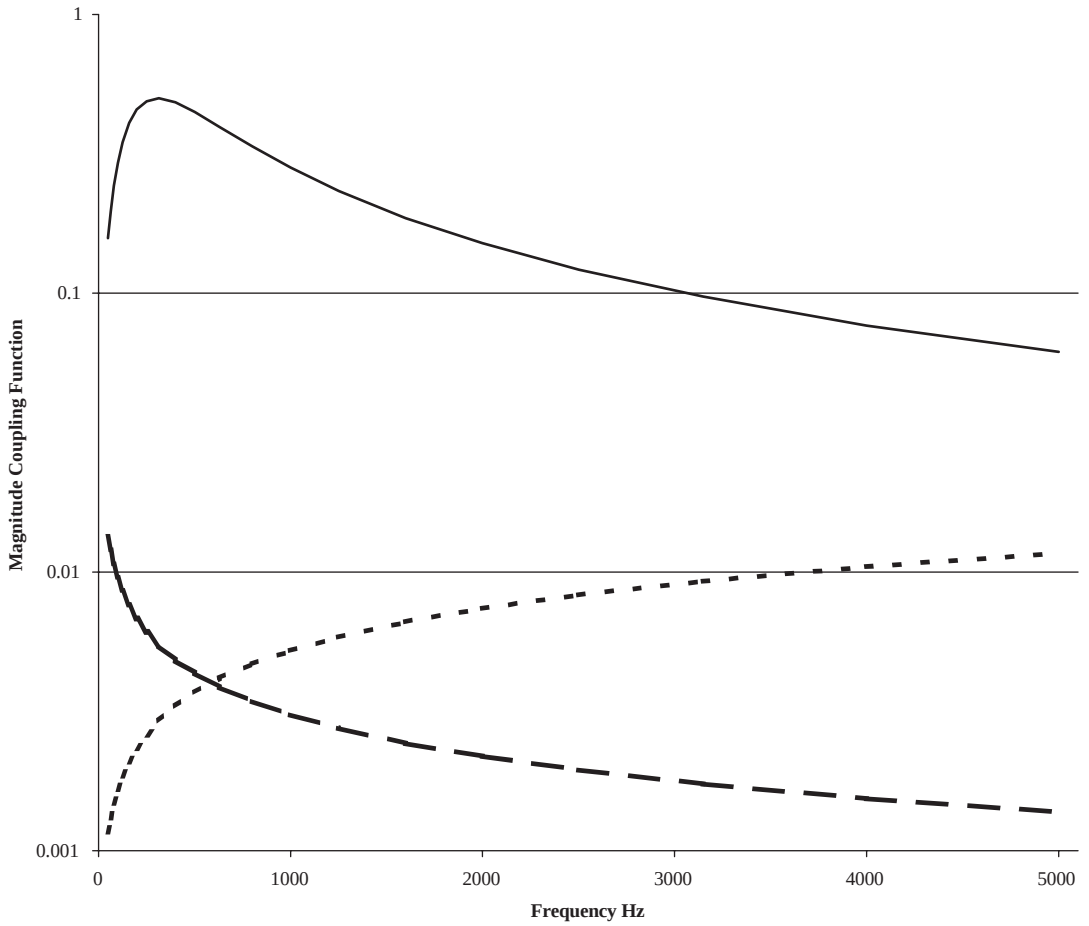

Fig. 4. Magnitude of coupling function between pipe and radiator: ————, x-direction (see Table 1): – – – –, y-direction; - - - - -, z-direction.

non-alignments in the system and the overall effect is that there is equal energy partitioning between all three components at frequencies greater than 800 Hz.

3.2. Three-pipe systems

In Fig. 5 are shown the normalised power transmission coefficients for a three-pipe system where the three pipes are in same plane with the radiator perpendicular (Fig. 1(b)). Results are similar to those of the two-pipe system. The power transmission coefficient for the input in the z-direction, $\gamma^{P_{rz}}_{P_{\text{in}z}}$ again is relatively low. However after two junctions, the values of power transmission coefficient converge with increase in frequency and are of the same order of magnitude at frequencies above 500 Hz.

In Fig. 6 are shown the normalised power transmission coefficients for three pipes, which are mutually perpendicular (Fig. 1(c)). In this case, the transmission coefficients are of the same order

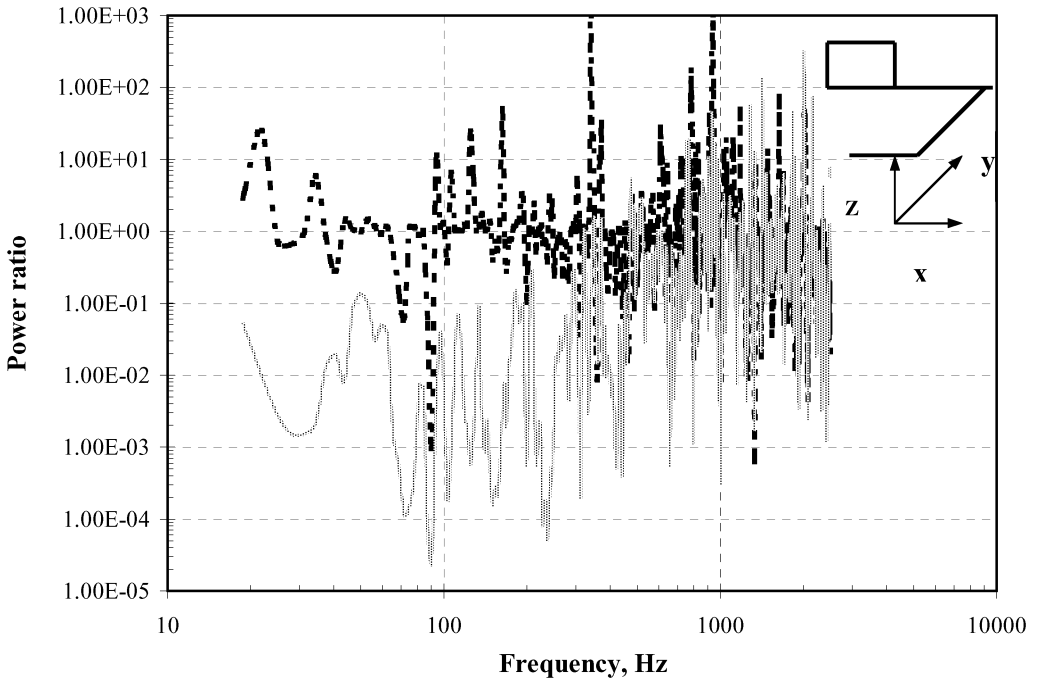

Fig. 5. Normalised transmission coefficients for three pipe system in the same plane: -----, $\gamma^{P_{ry}}_{P_{\mathrm{iny}}}/\gamma^{P_{rx}}_{P_{\mathrm{inx}}}$; ——, $\gamma^{P_{rz}}_{P_{\mathrm{inz}}}/\gamma^{P_{rx}}_{P_{\mathrm{inx}}}$.

of magnitude over the whole frequency range of 20 Hz–2.5 kHz but with large fluctuations about unity. Pipe resonances dominate the system response and it was not straightforward to extract the general trends. In addition, unavoidable imperfections in the construction of the pipe system gave rise to unquantifiable wave mode conversions. Therefore, an analytical model of idealised pipe systems was developed where the length of the connecting pipes could be varied stochastically to average out resonance effects and thereby allow the effect of number and geometry of pipe junctions on wave mode conversion to be studied.

4. Theoretical model of connected pipe systems

The theoretical model of connected pipe systems did not aim to simulate the experimental systems described in the previous section but to examine the role of the number and geometry of junctions on the wave mode transformation throughout pipe systems. By considering the pipes as idealised waveguides, the extraneous wave mode conversions, due to small misalignments and workmanship, could be eliminated from the study.

In structure-borne sound propagation along beams, rods and pipes there is, in addition to dissipative losses, attenuations due to impedance changes such as at junctions. The mechanism of wave transmission at junctions of rods is generally well understood [9,11,12] and formed the basis of the present analysis of connected pipes.

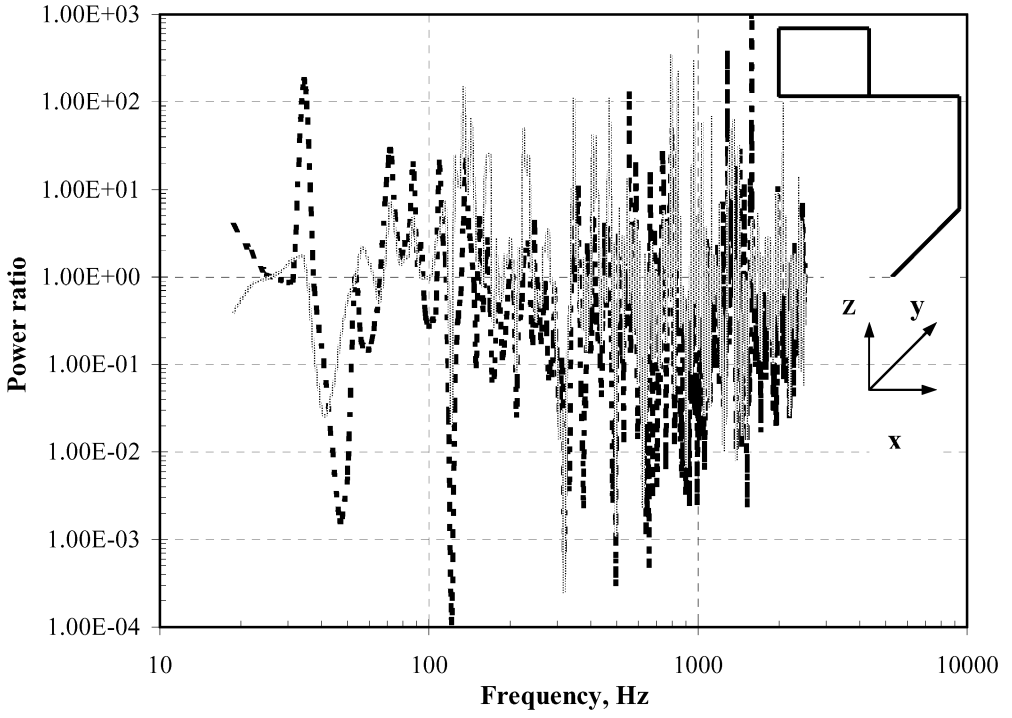

Fig. 6. Normalised transmission coefficients for three pipe system in three dimensions -----, $\gamma^{P_{ry}}_{P_{iny}}/\gamma^{P_{rx}}_{P_{inx}}$; ——, $\gamma^{P_{rz}}_{P_{inz}}/\gamma^{P_{rx}}_{P_{inx}}$.

Several simplifying assumptions were incorporated. At low non-dimensional frequencies $\left(\Omega = f/f_{\text{ring}} = \omega a/c_{LI} < 0.77\, h/a\right)$ the mobility of a pipe (a is the pipe radius and h the wall thickness) is very nearly the same as that of a square-section rod with a radius of gyration $a/\sqrt{2}$ [9]. Therefore, in the following analysis, square cross-sectional rods were considered. The effects of rotatory inertia and shear deformation were neglected and Euler–Bernoulli theory was assumed.

Pipe wall damping was neglected and the contained water was treated as a simple mass loading. In Fig. 7 is shown the predicted and measured point mobility at the end of a copper pipe with and without water. The predicted value was obtained from the expression for an infinite pipe contained in Table 1 [9]. The measurements were conducted on a 6 m pipe, which was buried in a sand box for a distance of 3.5 m. The fluctuations in measured values about the theoretical trend lines are the result of incomplete damping of bending vibrations by the sand. The fluid loading contributes little to the mobility of the pipe.

The model was simplified by assuming that the source and receiver pipes are semi-infinite; only the intermediate rods are finite. Therefore, the receiving system is a semi-infinite pipe, rather than the radiator in the experimental set-up. The power transmission coefficient is the ratio of the output power, in bending vibration away from the last junction, to the power incident at the first junction.

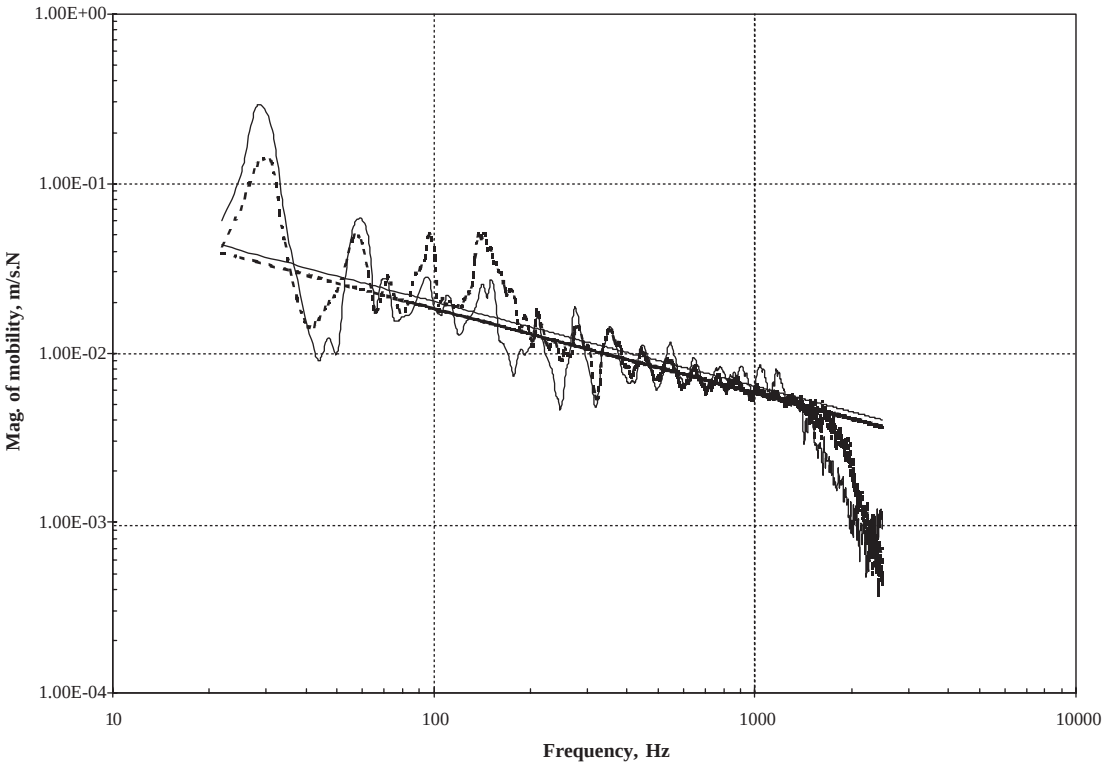

Fig. 7. Magnitude of mobility at the end of a copper pipe, with and without water. ----, predicted and measured without water; ——————, predicted and measured with water.

The input on the ith (semi-infinite) pipe can be an incident longitudinal wave, given by

$$L_i = l_i \mathrm{e}^{-\mathrm{j}k_{Li}x_i}\mathrm{e}^{\mathrm{j}\omega t}, \tag{6}$$

where l_i is the complex amplitude coefficient and $k_{Li} = \omega\sqrt{\rho_i/E_i}$ is the longitudinal wave-number, ω is the angular frequency, ρ_i is the material density and E_i is the Young's modulus.

An incident torsional wave is given by

$$T_i = t_i \mathrm{e}^{-\mathrm{j}k_{Ti}x_i}\mathrm{e}^{\mathrm{j}\omega t}, \tag{7}$$

where t_i is the complex amplitude coefficient and $k_{Ti} = \omega\sqrt{\rho_i J_i/C_i}$ is the torsional wave number, J_i is the polar moment of inertia of the cross-section of the rod and C_i is the torsional rigidity.

An incident bending wave is given by

$$B_i = \left(b_i \mathrm{e}^{-\mathrm{j}k_{B_i}x_i} + b_{ni}\mathrm{e}^{-k_{B_i}x_i}\right)\mathrm{e}^{\mathrm{j}\omega t}, \tag{8}$$

where b_i is the complex amplitude coefficient of travelling component and b_{ni} is that of the nearfield. The wave number $k_{B_i} = \sqrt{\omega/(\rho_i S_i/B)^{1/4}}$, S_i the area of the pipe cross-section and B is the bending stiffness.

The power of a bending wave of displacement amplitude b_i is given by

$$P_{B_i} = \frac{S_i \rho_i \omega^3}{k_{B_i}} |b_i|^2. \tag{9}$$

The power of a longitudinal wave of displacement amplitude l_i is given by

$$P_{L_i} = \frac{1}{2} \frac{S_i \rho_i \omega^3}{k_{L_i}} |l_i|^2. \tag{10}$$

The power of a torsional wave is given for completeness, as

$$P_{T_i} = \frac{1}{2} \frac{J_i \rho_i \omega^3}{k_{T_i}} |t_i|^2. \tag{11}$$

Torsional waves were not considered as inputs but were included as intermediate and output waves. Since the model assumes zero internal losses, the power into the system must equal the power out.

4.1. Theoretical two-pipe system

The simplest system of connected pipes for analysis consists of two semi-infinite pipes at a right angle, shown in Fig. 8. When a wave, either a longitudinal or one of two polarised bending waves, arrives at junction, two reflected waves are generated on pipe 1 and two transmitted waves on pipe 2. When a bending wave arrives at the junction with displacement in the plane of the two pipes, it gives rise to: a reflected bending wave with in-plane displacement; a reflected longitudinal wave; a transmitted in-plane bending wave; a transmitted longitudinal wave on pipe 2. The displacements on the two pipes are given by

$$\begin{aligned}
y_{1,B} &= B_{in}\left(\mathrm{e}^{\mathrm{j}k_B x_1} + B_{1r}\mathrm{e}^{-\mathrm{j}k_B x_1} + B_{1rn}\mathrm{e}^{-k_B x_1}\right)\mathrm{e}^{\mathrm{j}\omega t},\\
x_{1,L} &= B_{in}(L_{1r}\mathrm{e}^{-\mathrm{j}k_L x_1})\mathrm{e}^{\mathrm{j}\omega t},\\
y_{2,B} &= B_{in}(B_{2t}\mathrm{e}^{-\mathrm{j}k_B x_2} + B_{2tn}\mathrm{e}^{-k_B x_2})\mathrm{e}^{\mathrm{j}\omega t},\\
x_{2,L} &= B_{in}(L_{2t}\mathrm{e}^{-\mathrm{j}k_L x_2})\mathrm{e}^{\mathrm{j}\omega t}.
\end{aligned} \tag{12}$$

For simplicity, B_{in} set to unity and the time dependency term $\mathrm{e}^{\mathrm{j}wt}$, which is common to all wave expressions, can be excluded.

The boundary conditions at the junction are given by the continuity equations

$$\begin{aligned}
&\textit{Displacement}: && y_{1,B|_{x_1=0}} = x_{2,L|_{x_2=0,}}\\
& && y_{2,B|_{x_2=0}} = -x_{1,L|_{x_1=0,}}\\
&\textit{Slope}: && w_{1,B|_{x_1=0}} = w_{2,B|_{x_2=0,}}\\
&\textit{Moments}: && M_{1,B|_{x_1=0}} = -M_{2,B|_{x_2=0,}}\\
&\textit{Force}: && F_{1,B|_{x_1=0}} = -F_{2,L|_{x_2=0,}}\\
& && F_{2,B|_{x_2=0}} = F_{1,L|_{x_1=0.}}
\end{aligned} \tag{13}$$

Substituting Eq. (12) into Eq. (13) yields a set of simultaneous equations, which can be solved to give the powers in Eq. (9)–(11) and thus the transmission coefficients in Eq. (1).

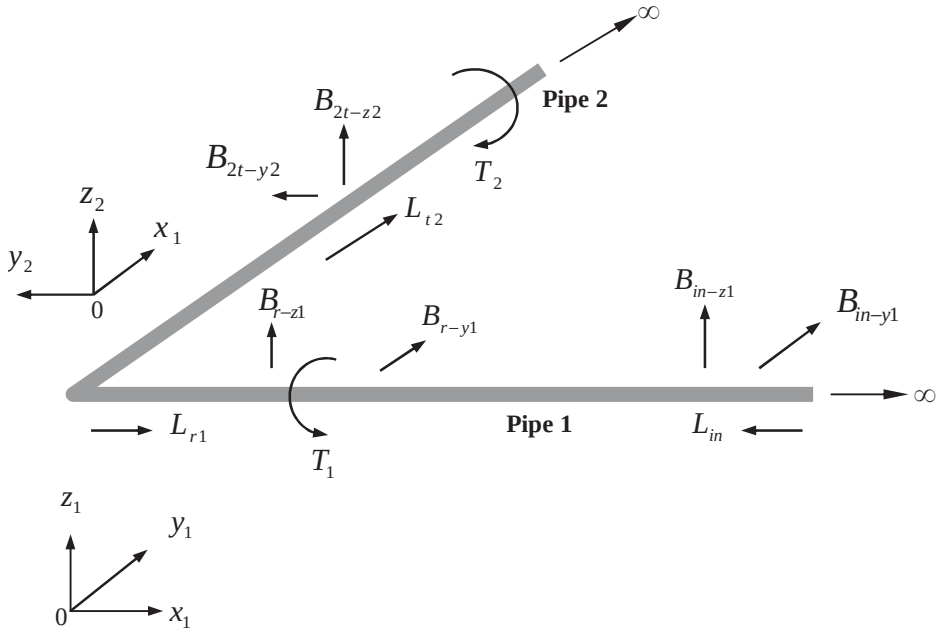

Fig. 8. Coordinate system and modes of vibration for a junction of two semi-infinite pipes.

In Fig. 9(a) are shown the four power transmission coefficients for two copper rods, $S = 6.25 \times 10^{-4}\,\mathrm{m}^2$, $E = 12.5 \times 10^{10}\,\mathrm{Nm}^{-2}$. The four power transmission coefficients were calculated over the frequency range of 10 Hz–4 kHz in increments of 10 Hz. A similar procedure applies for a bending wave incident with out of plane displacement (Fig. 9 (b)) and a longitudinal wave arriving at the junction (Fig. 9 (c)). The system is non-resonant and all values are monotonic functions of frequency. Wave transformation increases with frequency although that between bending and torsion is relatively small and slowly varying with frequency.

4.2. Theoretical three-pipe system

Consider a three-pipe system, two semi-infinite pipes connected at right angles through a finite length pipe, with all pipes in the x–y plane (Fig. 10). For a bending wave incident with displacement in the plane of the pipes (B_{y1}), the displacements on the three pipes are given by

$$\begin{aligned} y_{1,B} &= \mathrm{e}^{\mathrm{j}k_B x_1} + B_{1r}\mathrm{e}^{-\mathrm{j}k_B x_1} + B_{1rn}\mathrm{e}^{-k_B x_1}, \\ x_{1,L} &= L_{1r}\mathrm{e}^{-\mathrm{j}k_L x_1}, \\ y_{2,B} &= B_{2t}\mathrm{e}^{-\mathrm{j}k_B x_2} + B_{2tn}\mathrm{e}^{-k_B x_2} + B_{2r}\mathrm{e}^{\mathrm{j}k_B x_2} + B_{2rn}\mathrm{e}^{k_B x_2}, \\ x_{2,L} &= L_{2t}\mathrm{e}^{-\mathrm{j}k_L x_2} + L_{2r}\mathrm{e}^{\mathrm{j}k_L x_2}, \\ y_{3,B} &= B_{3t}\mathrm{e}^{-\mathrm{j}k_B x_3} + B_{3tn}\mathrm{e}^{-k_B x_3}, \\ x_{3,L} &= L_{3t}\mathrm{e}^{-\mathrm{j}k_L x_3}. \end{aligned} \tag{14}$$

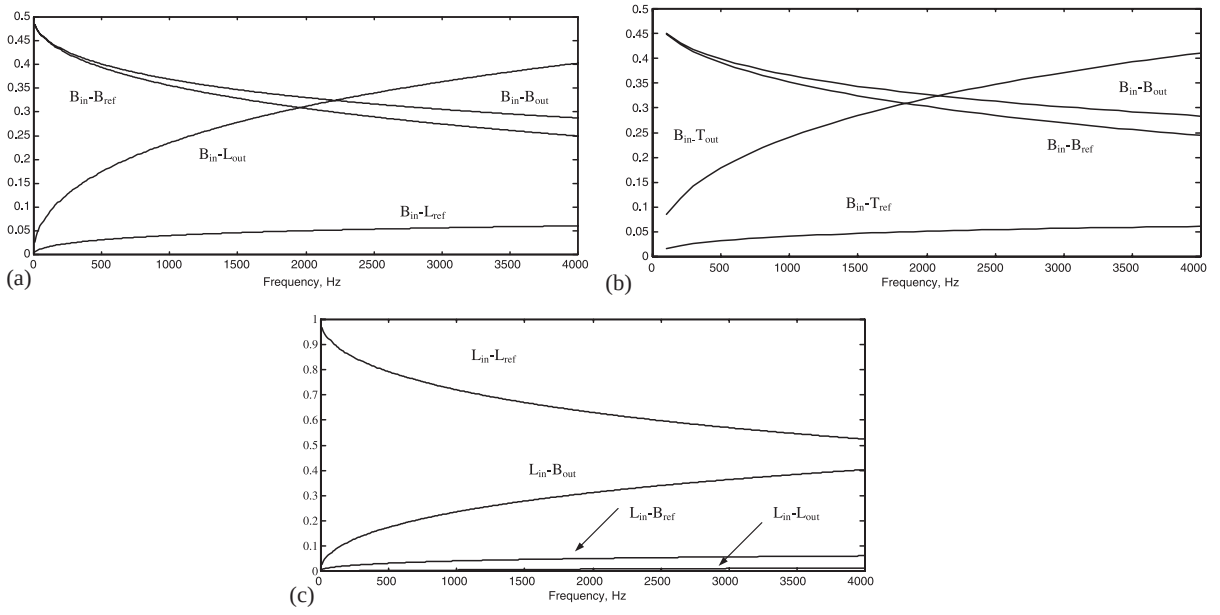

Fig. 9. Power transmission coefficients at a corner junction of semi-infinite pipes: (a) bending wave incident with in plane displacement, (b) out of plane bending wave, (c) longitudinal wave.

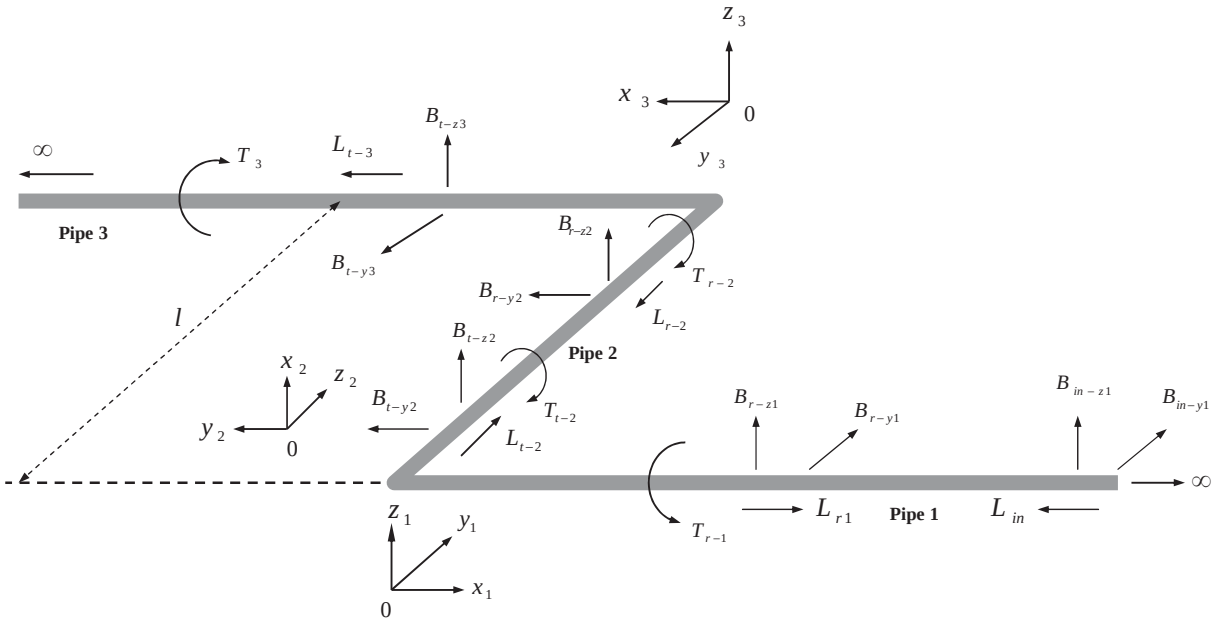

Fig. 10. Coordinate system and modes of vibration for three pipes in the same plane.

The output power is carried by a polarised bending wave with displacement in the plane of the pipes ($B_{y1}-B_{y3}$) and by a longitudinal wave ($B_{y1}-L_3$). A solution for the power transmission coefficients is given for a central pipe of length 3 m in Fig. 11(a). It can be seen that there are several peak values above unity in the frequency range above 700 Hz. This is the result of computational overflows and underflows at resonant frequencies in this loss-less and thus highly resonant system. The results are otherwise stable and a power balance can be assumed.

In Fig. 11(b) are shown the power transmission coefficients for the same system but for an out-of-plane bending wave input (B_{z1}). Here, torsional waves are generated, given by

$$\begin{aligned} t_1 &= T_{1r}\mathrm{e}^{-\mathrm{j}k_T x_1}, \\ t_2 &= T_{2t}\mathrm{e}^{-\mathrm{j}k_T x_2} + T_{2r}\mathrm{e}^{\mathrm{j}k_T x_2}, \\ t_3 &= T_{3t}\mathrm{e}^{-\mathrm{j}k_T x_3}. \end{aligned} \tag{15}$$

The output power is carried from the system by torsional ($B_{z1}-T_3$) and out of plane bending waves ($B_{z1}-B_{z3}$). In Fig. 11(c) are the transmission coefficients for a longitudinal wave incident (L_1). Incident torsional waves were not considered since it had been demonstrated previously [6] that pumps do not impart significant powers through moments, although torsional waves are

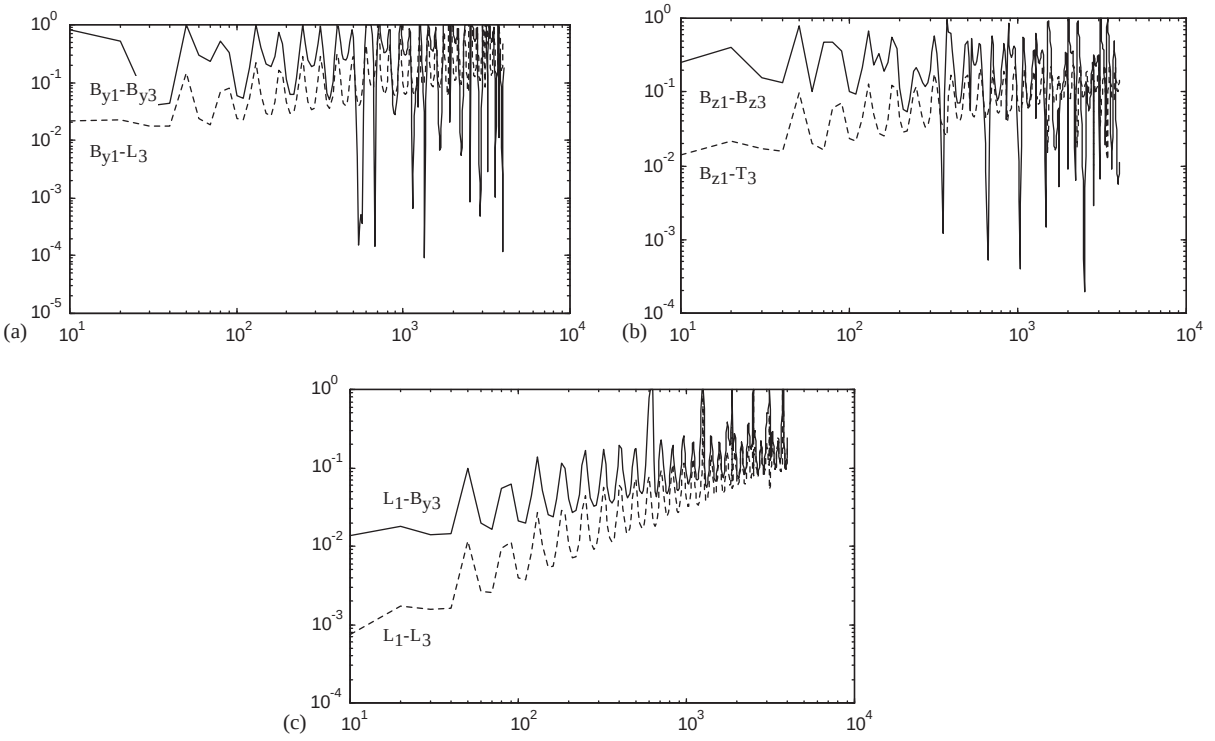

Fig. 11. Power transmission coefficients for three pipes in the same plane: (a) bending wave B_{y1} incident with displacement in plane: ————, bending wave B_{y3} out; ------- longitudinal wave L_3 out; (b) out of plane bending wave B_{z1} incident: ————, bending wave B_{z3} out; ------- torsional wave T_3 out; (c) longitudinal wave L_1 in:————, longitudinal wave L_3 out ;·-·-·-·- bending wave B_{y3} out.

included as part of the wave mode conversion and transmission along the intermediate pipes. In all cases, the power transmission coefficients increase with frequency and display convergence. The trends are partially masked by fluctuations due to resonances in the intermediate pipe.

In most domestic piped water systems, the pipes are not in the same plane but in three dimensions (Fig. 12). For any wave input, there will be four waves generated on each pipe: longitudinal, torsional and two polarised bending waves. All contribute to the power carried from the system (B_{y3}, B_{z3}, L_3, T_3) as well, of course, as the reflected waves (B_{y1}, B_{z1}, L_1, T_1). The power

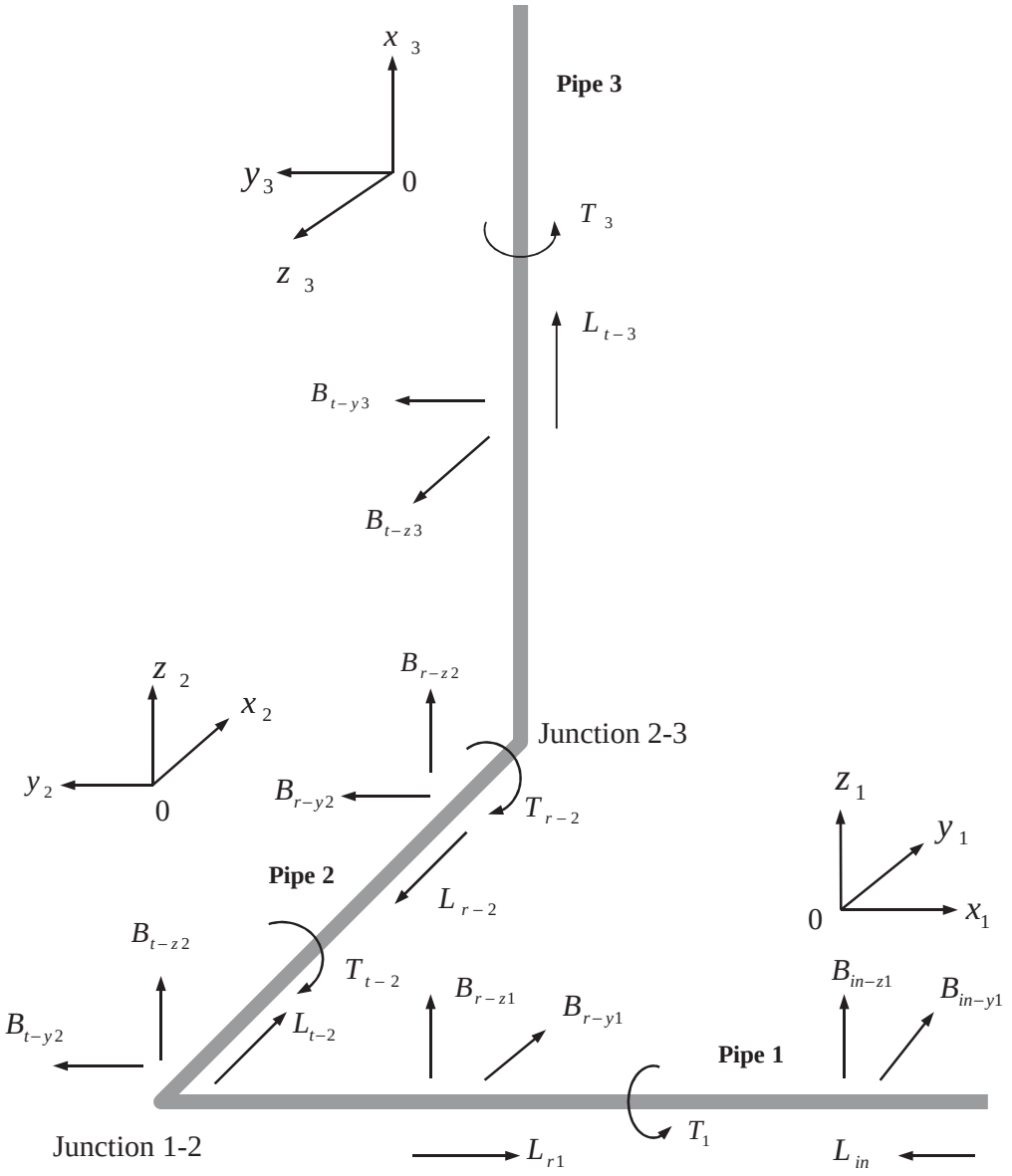

Fig. 12. Coordinate system and modes of vibration for a three mutually perpendicular pipes.

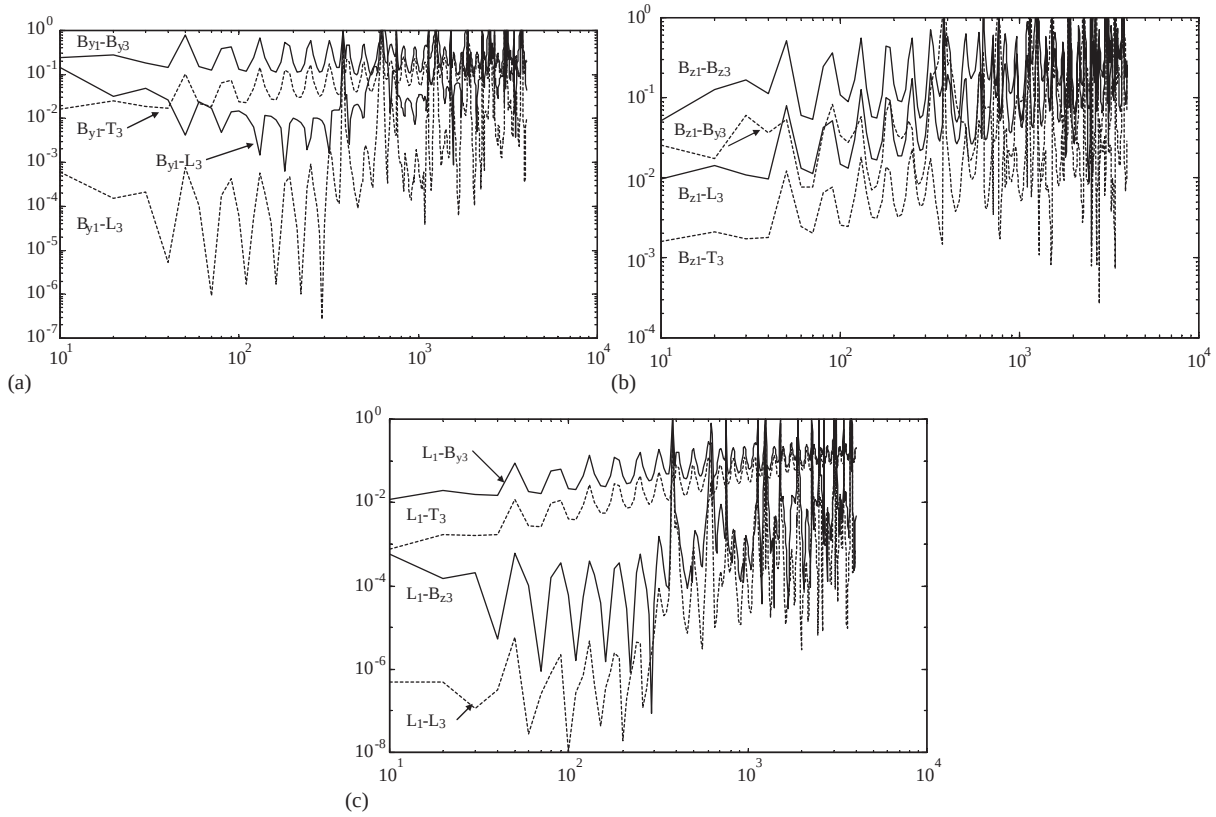

Fig. 13. Power transmission coefficients for a three mutually perpendicular pipes: (a) bending wave B_{y1} incident, (b) bending wave B_{z1} incident, (c) longitudinal wave L_1 incident.

transmission coefficients, for an incoming bending wave, polarised in the y-direction (B_{y1}), are shown in Fig. 13(a). Again, there are some values greater than unity because of the increased computational demands of this model and some instability in the calculation. Fig. 13(b) shows results for a bending wave incident, with displacement in the z direction (B_{z1}) and Fig. 13(c) is for a longitudinal wave incident (L_1). In all cases, values converge with increase in frequency, indicating a trend towards energy equipartition.

5. Stochastic model of a finite connecting pipe

In order to extract the general effect of the junctions, the length of the middle pipe in a three pipe system (see Fig. 12 for coordinate system) was varied and values of average power ratios obtained. In domestic central heating systems, most of the pipe lengths are within the range 0.5 and 4 m. In this study, 100 values, between 0.5 and 4 m, were selected randomly. In order to extract the trend in bending power transmission coefficient, the log-average values of power transmission coefficient were obtained, along with the standard deviations, for the sample of 100

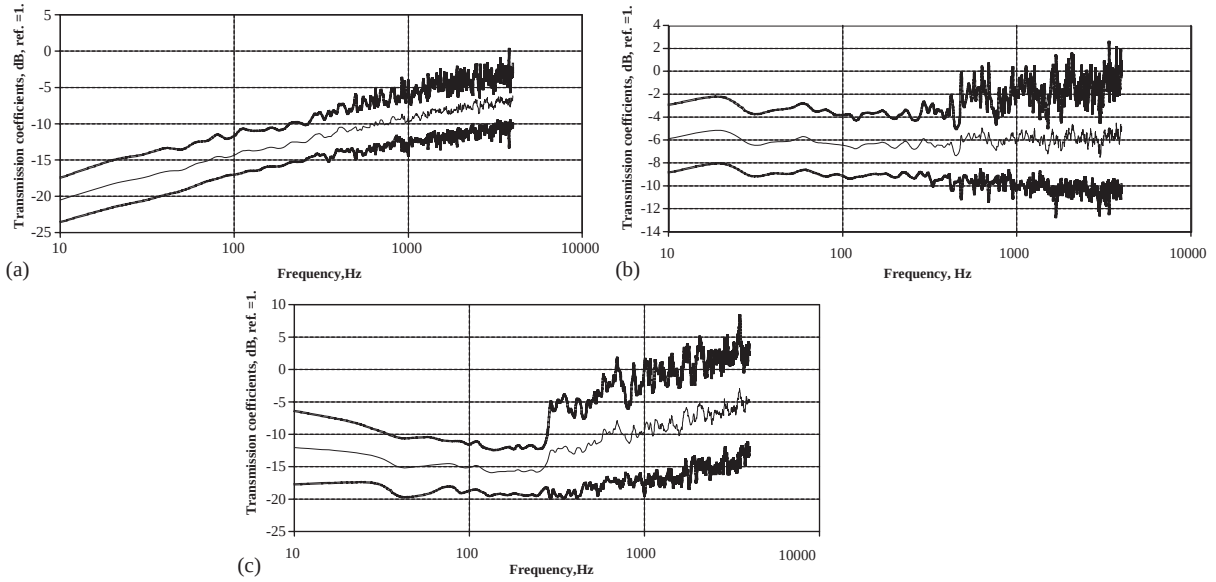

Fig. 14. Average values and standard deviations of power transmission coefficients for 100 random values of central pipe length in three mutually perpendicular connected pipes, for bending wave B_{y3} out: (a) $\gamma^{B_{y3}}_{L_{in}} \pm \sigma_s$, (b) $\gamma^{B_{y3}}_{B_{y1}} \pm \sigma_s$, (c) $\gamma^{B_{y3}}_{B_{z1}} \pm \sigma_s$.

randomly generated pipe lengths. In Figs. 14 are shown the average values of transmission coefficient, plus and minus one standard deviation, for an outgoing bending wave polarised in the y-direction, for three possible input waves. In Fig. 15 are shown values for an outgoing bending wave polarised in the z-direction. In Fig. 16, the average values are compared. For each input wave, the longitudinal or either of the two polarised bending waves, the wave mode conversion is sufficient for equipartioning of the energy at high frequencies, in most cases. It is reasonable to assume that a more complicated model of more than two junctions will cause more wave mode conversion with equipartitioning at a lower frequency than indicated in Fig. 13.

6. Concluding remarks

For pipe dimensions typical of domestic systems and for the frequency range of interest, the circulation pumps generate plane waves in the liquid and longitudinal and polarised bending waves in the pipes.

Idealised pipe systems were considered, with no imperfections or misalignments. It was shown that for three mutually perpendicular connected pipes the contributions to far-field bending fields of the three components of force generated by a pump converge to equal values at about 2 kHz.

In real pipe systems, increased wave mode conversions occur due to misalignments and imperfections in workmanship. Equipartitioning of energy occurs at lower frequencies. For the three-pipe–radiator system measured, the contributions to the far-field bending field of the three components of force were the same over the whole frequency range of interest.

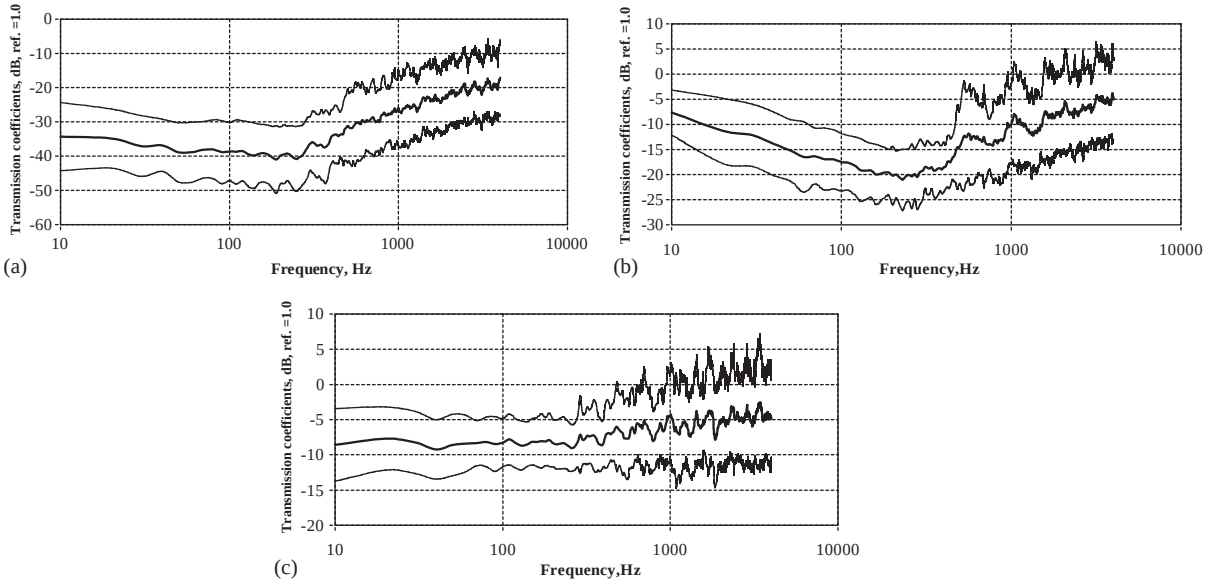

Fig. 15. Average values of power transmission coefficients and standard deviations for bending wave B_{z3} out: (a) $\gamma^{B_{z3}}_{L_{in}} \pm \sigma_s$, (b) $\gamma^{B_{z3}}_{B_{y1}} \pm \sigma_s$, (c) $\gamma^{B_{z3}}_{B_{z1}} \pm \sigma_s$.

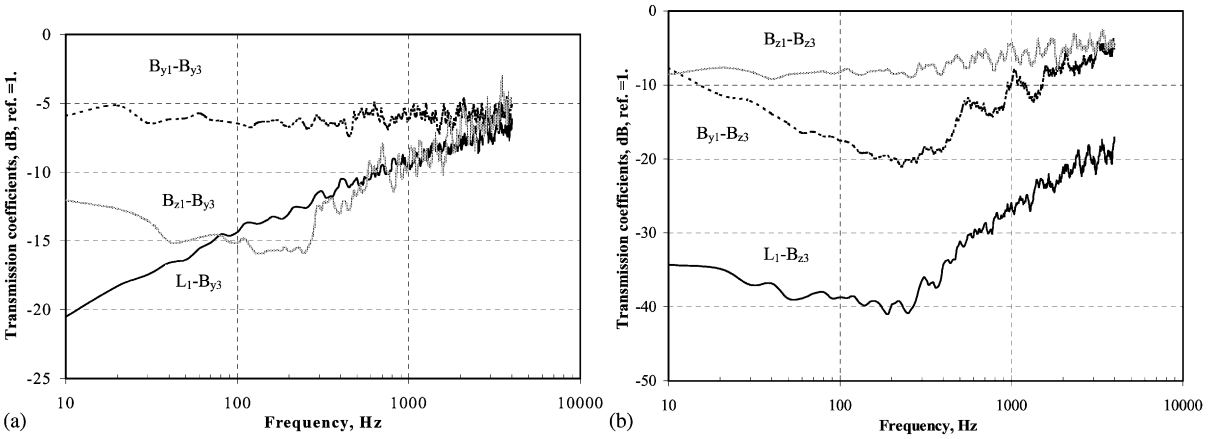

Fig. 16. Average values of power transmission coefficients for 100 random values of central pipe length in three mutually perpendicular connected pipes: (a) bending wave B_{y3} out, (b) bending wave B_{x3} out.

It follows that the most influential component of input power from a pump is simply the largest, irrespective of component direction. Domestic installations are likely to be in three dimensions, involving several junctions and other discontinuities. This, and inevitable imperfections in workmanship will contribute to wave mode conversion and thus enhanced mixing of the contributions of the components of the input power.

Acknowledgements

The authors gratefully acknowledge the financial support of this work by the Engineering and Physical Sciences Research Council of the UK.

References

[1] N. Qi, A.T. Moorhouse, B.M. Gibbs, Investigation of appropriate measurements to characterize small domestic central heating pumps as structure-borne noise sources, *Proceedings of Euro-noise 98*, vol. 1, 1998 pp. 395–400.
[2] ISO 10767-1, Hydraulic fluid power—determination of pressure ripple levels generated in systems and components, 1996.
[3] ISO/CD 1690-2, Hydraulic fluid power—test code for the determination of sound power levels of pumps using sound intensity techniques, 1999.
[4] ISO 3822, Acoustics-laboratory tests on noise emission from appliances and equipment used in water supply installations, 1983.
[5] K. Trdak, A. Badie-Cassagnet, G. Pavic, Characterisation of small circulation pumps as sources of vibroacoustic energy, *Proceedings Internoise* 2000, 4-2389, 4pp.
[6] N. Qi, B.M. Gibbs, Circulation pumps as structure-borne sound sources: emission to semi-infinite pipe systems, *Journal of Sound and Vibration* 264 (2003) 157–176.
[7] F.J. Fahy, R. Pierry, Application of the cross-spectral density to a measurement of vibration power flow between connected plates, *Journal of the Acoustical Society of America* 62 (1976) 1297–1298.
[8] F.J. Fahy, *Sound and Structural Vibration. Radiation, Transmission and Response*, Academic Press, London, 1985.
[9] L. Cremer, M. Heckl, E.E. Ungar, *Structure-Borne Sound*, Springer, Berlin, 1973.
[10] J.M. Mondot, B.A.T. Petersson, Characterisation of structure-borne sound sources: the source descriptor and the coupling function, *Journal of Sound and Vibration* 114 (3) (1987) 501–518.
[11] J.P. Lee, H. Kolsky, The generation of stress pulses at the junction of two non-collinear rods, *Journal of Applied Mechanics* 39 (1972) 809–813.
[12] B.M. Gibbs, J.D. Tattersall, Vibrational energy transmission and mode conversion at a corner-junction of square section rods, *Transactions of ASME* 109 (1987) 348–355.
[13] J.L. Guyader, E. Parizet, Uncertainty of vibroacoustic behaviour of industrially identical structures, *Proceedings of the Fifth International Congress on Sound and Vibration*, Adelaide, 1997.